Journal of Complementary Medicine Research, ISSN: 2577-5669 Vol. 11, No.5, 2020 (pp.266-280)

JOURNAL OF COMPLEMENTARY MEDICINE RESEARCH

RESEARCH ARTICLE WWW.JOCMR.COM

Sensor Fault Tolerant Air-Fuel Ratio Control in Internal Combustion Engines via Artificial Neural Networks and Sliding Mode Control

[1]BALABHADRA NAGARAJU,[2]JITHENDER BANDARI,[3]UMASHANKAR YADAGIRI,[4]BOLLEPALLI HARI HARA VISHNU,[5]AMBALA VENKATESH

[123]Assistant Professor, [4,5]B. Tech Student

Department Of Mechanical Engineering

Vaagdevi College of Engineering, Warangal, Telangana.

ABSTRACT:

This study presents a novel approach to managing the air-fuel ratio in internal combustion engines (ICEs) by integrating an artificial neural network (ANN) with sliding mode control (SMC) to enhance system robustness against sensor failures. Accurate air-fuel ratio control is crucial for optimizing engine performance, fuel efficiency, and emissions. However, sensor malfunctions can significantly disrupt the control process, leading to poor engine operation and increased emissions. This research proposes a hybrid control strategy that employs ANN for precise estimation of the optimal air-fuel ratio and SMC to ensure stability and robustness in the presence of sensor faults. The ANN is trained on a comprehensive dataset representing various operating conditions of the engine, enabling it to adaptively predict the required air-fuel ratio. Meanwhile, the SMC design effectively mitigates the impact of sensor failures by maintaining control system performance through variable gains and robust feedback mechanisms. Simulation results demonstrate that the proposed method significantly improves air-fuel ratio control accuracy and system resilience compared to traditional control strategies. This research contributes to the advancement of intelligent control systems for internal combustion engines, paving the way for enhanced performance and reduced environmental impact in automotive applications.

Keywords

Artificial neural network, sliding mode control, air-fuel ratio control, Lyapunov stability, and fault-tolerant control.

I. Introduction

The management of air-fuel ratio in internal combustion engines (ICEs) is critical for optimizing engine performance, ensuring fuel efficiency, and minimizing harmful emissions. The air-fuel ratio, defined as the ratio of air mass to fuel mass in the combustion process, directly influences the combustion efficiency and the overall operation of the engine. An optimal air-fuel mixture is essential for achieving complete combustion, reducing exhaust emissions, and enhancing power output. As automotive technology continues to evolve, the need for advanced control strategies that can adapt to varying operational conditions and potential system faults has become increasingly important.

Traditional control methods for air-fuel ratio management often rely on fixed algorithms or simplistic control strategies that may not effectively accommodate the dynamic nature of engine operation or respond adequately to sensor malfunctions. Sensor failures can lead to significant deviations in the measured air-fuel ratio, resulting in poor engine performance, increased fuel consumption, and higher emissions. Consequently, developing robust control mechanisms capable of maintaining optimal air-fuel ratio management despite sensor uncertainties is a critical challenge in modern engine control systems.

This study proposes an innovative approach that integrates artificial neural networks (ANNs) with sliding mode control (SMC) to enhance air-fuel ratio management in internal combustion engines while ensuring fault tolerance against sensor failures. The ANN serves as a predictive model that learns and adapts to various engine operating conditions, providing real-time estimates of the optimal air-fuel ratio. In parallel, the SMC framework offers robustness and stability, effectively counteracting the effects of sensor faults through dynamic feedback mechanisms.

By employing this hybrid control strategy, this research aims to improve the accuracy of air-fuel ratio management, enhance engine performance, and reduce environmental impact. The findings of this study are expected to contribute significantly to the development of intelligent control systems in the automotive industry, providing a pathway toward more efficient and reliable internal combustion engines.

Table 1. List of abbreviations.

Abbreviation	Explanation
FTC	Fault-tolerant control
HFTCS	Hybrid fault-tolerant control system
PFTCS	Passive fault-tolerant control system
AFTCS	Active fault-tolerant control system
SMC	Sliding mode control
ANN	Artificial neural network
AFR	Air-fuel ratio
AR	Analytical redundancy
IC Engine	Internal combustion engine
MVEM	Mean value engine model
MAP	Manifold air pressure.
EGO	Exhaust gas oxygen sensor

and properties, FTCS is divided into two major categories: active and passive. Some symbols and abbrevia- tions related to HFTCS are listed in Tables 1 and 2, respectively.

In active fault-tolerant system (AFTCS), the fault detection and isolation (FDI) unit is designed to detect the fault in the online mode and it isolates faulty val- ues.4–6 The FDI unit compares the values of the actual sensors with the estimated values being generated from the observer for a residual generation. The fault in the component is declared when the residual value exceeds its predefined limiting value. The controller is then reconfigured to adapt according to the current faulty conditions after fault detection and isolation, with little output deterioration.7,8 Unlike AFTCS, passive fault-tolerant system (PFTCS) may not need a dedicated FDI unit, and any fault in the design stage of the con- trol system is considered beforehand in the offline mode.9–11 PFTCS is, therefore, very swift than AFTCS due to lesser computational cost, but it has the draw- back to deal with the faults only that were considered during the construction of the controller.12,13 A combi- nation of all these approaches is also built by integrat- ing both types, namely hybrid fault-tolerant control system (HFTCS). In protective and safety applications, the hybrid system can rapidly respond to faults with the PFTCS property and later optimize itself with the AFTCS property.14–16 In Amin,14 the HFTCS has been proposed with Kalman Filters in the active part and a high-gain PI controller in the passive part. This algorithm was limited to the linear range of the highly non- linear sensors of the AFR control system. In Su et al.,15 the HFTCS was proposed for the sensors of the distilla- tion column without using any intelligent control or data-driven technique. In Wang et al.,16 the HFTCS was proposed for the uncertain networked control sys- tems under a discrete event-triggered communication scheme that was not applied to the process plant.

A comprehensive study of the FTCS has been mentioned for the nonlinear system in Li17 for various fault

Table 2. List of symbols.

Symbol	Explanation
m_{air}	Mass of air
m_{fuel}	Mass of fuel
T_{in}	Input temperature
P_m	Manifold pressure
v_{in}	Input volume
$\dot{m}_{th}$	Mass flow through the valve
$\dot{m}_{Cyl}$	Mass flow into cylinders
R	Gas constant
N_e	Engine speed
e_x	Residual
ϕ_{th}	Throttle opening position
C_d	Discharge coefficient
$S_{es}(\phi_{th})$	True throttle opening position
γ	Heat-ratio of air
τ_f	Fuel vapor process
$\dot{m}_{fi}(t)$	Fuel flow injection
$\dot{m}_f(t)$	Fuel flow into cylinders
$\dot{m}_{fv}$	Vapor fuel flow
$\dot{m}_{ff}(t)$	Liquid mass fuel flow
$\lambda(t)$	Lambda sensor
τ_λ	Time delay
y_d	Desired output
y	Actual output
u	Actual Input
x_1/x_2	State variables
α/β	Parameters of engine
$\bar{x}_1/\bar{x}_2$	Estimated values of observer design
$\bar{y}$	Estimated output
E	Root mean square error
η	Learning rate
$\Xi_i(x)$	Base function
Δ_i	Unknown constant parameter
S_{ol}	Conventional sliding mode design
U_o	Maintain the known terms
M_i	Unstructured uncertainties
Θ_i	Structured faults
Θ_1 and Θ_2	Over and underflow

scenarios. In Yang et al.,18 the non-linear hybrid FTCS design was established for feature extraction, and the actuator fault adjustment control was applied. The arti- ficial neural networks (ANN) technique was applied for the switched-type nonlinear systems in Tang et al..19 For a single-tank system with system faults and process disturbances, a fuzzy logic-based passive fault-tolerant control method was proposed in Patel and Shah.20 In Murtaza et al.,21 a super-twisting control-based unified FDI and FTC system for the air path of diesel engines is reported. Kalman Filters (KFs) were also used in the FDI architecture of gas turbines for faulty sensor esti- mation22,23 consisting of both hardware and analytical redundancies.

Artificial neural networks

The artificial neural network (ANN) includes the con- cept of artificial intelligence, whose aim is to allow the systems to learn from experience. ANN works on the same logic as a human brain. It is a smart and modern approach to data-driven problems.24 This non-linear technique is used in real-time problems like the model- ing of the engine because the engine is a highly non- linear system and ANN provides an optimal solution for such highly nonlinear problems.25–27 The architec- ture of the ANN is shown in Figure 1.

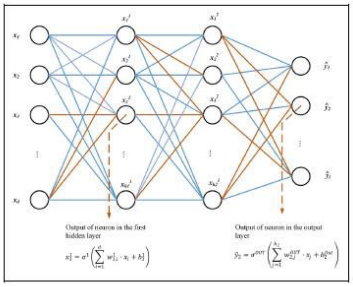

Figure 1. The architecture of ANN.[24]

ANN performs a data-parallel function, therefore, sequential simulations are easier than standard systems. The ANN works with both forward and backpropaga- tion. Its multi-layer perceptron model is known as a backpropagation neural network (BPNN).28–30 The input is in the form of samples and is treated with dif- ferent multiple hidden layers before the required output is mapped through this input. In Gao et al.,30 FTC architecture was proposed with an adaptive neural net- work for

Multi-Input Multi-Output (MIMO) systems. In Wang et al.,31 the ANN is utilized with a backpropa- gation strategy for the fault-tolerant control system. An adaptive neural network for the unmolded dynamic solution is proposed in Yin et al.32 The dataset is mapped to real numbers, that is, (x, y) where x repre- sents the selected feature and y translates the health state to this feature. ANN is described in terms of mathematical form is,

$$a_j^l = \sigma \sum_k w_{jk}^l a_k^{l-1} + b_j^l \qquad (1)$$

where wl represents the weight matrix inputs, bl shows the bias vector for layers l, and al is activation vector with the activation elements al.

Sliding mode control

Robust control is a control system architecture tech- nique that can allow systems to manage faults as long as the faults stay within the predefined limits.33,34 Robust control systems are static rather than dynamic and do not adjust to their conditions. For example, a high-gain feedback system is a robust control system due to its high gain, and changes in the other para- meters prove negligible due to its robustness. Sliding mode control (SMC) is derived from a variable struc- ture control system that mostly incorporates various control structure features and performs better than existing classical control structures.35,36 There are two phases in the SMC design as represented in Figure 2.

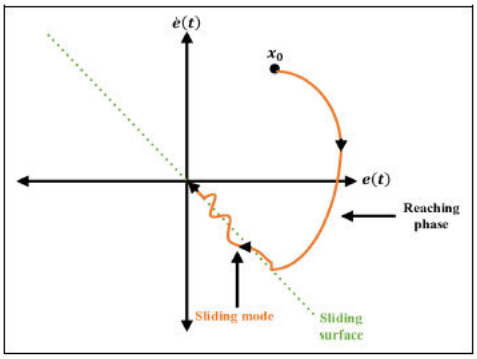

Figure 2. Sliding mode control.[33]

SMC triggers chattering in the actuator because of the rapid switching, therefore, a higher-order SMC named as super twisting algorithm is used to reduce the chattering problem.37 It is a non-linear technique with exceptional robustness properties. In practical terms, SMC facilitates non-linear processes that are subject to large model uncertainties. SMC will form the passive part in our proposed HFTCS to react instantly to faults.38

A customizable surface needs to be built in the first phase. The second phase should be planned to ensure that the system converges to the sliding surface for a minimum time. The phenomenon in which the motion takes place on a sliding surface is known as a sliding mode.38

AFR control of IC engines

The internal combustion engine is a type of heat enginein which the combustion of air and fuel takes place inside the cylinder and is used as the direct motive force. These engines transform the chemical energy of a fuel into thermal energy and use this energy to produce mechanical work. Its two main types are known as Spark Ignition (SI) and Compression Ignition (CI). In SI engines, the combustion takes place with the help of spark plugs, while in CI engines, the heat of compres- sion is used for combustion.39

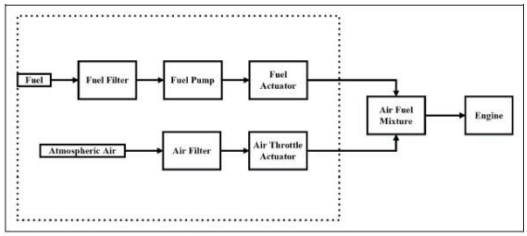

Figure 3. Air-fuel ratio control of an SI IC engine.[39]

The term air-fuel ratio (AFR) is defined as a mixture ratio of proper fuel and air in the combustion chamber and it is widely used to enhance the reliability and effi- ciency of the IC engine. Its mathematical expression can be written as:

$$AFR = \frac{m_{air}}{m_{fuel}} \qquad (2)$$

where mair represents the mass of the air and mfuel rep- resents the mass of the fuel. The equation of AFR for gasoline mixture is,

$$25O_2 + 2C_8H_{18} \rightarrow 16CO_2 + 18H_2O + Energy \qquad (3)$$

According to this equation, AFR is said to be the stoi- chiometric ratio with a value of 14.6:1 for gasoline fuel and is desirable for optimum combustion, fuel energy savings, and reduced emissions levels. If the mixture has AFR greater than 14.6:1, it is known as a lean mix- ture with greater air than fuel. A mixture with lesser than 14.6:1 is termed a rich mixture with greater fuel than oxygen. However, both of them are considered to be harmful to the engine's performance and life as it decreases their efficiency. The value of AFR is different for various categories of fuels. For example, methanol values are 6.47:1, 9:1 for ethanol, and 34.3:1 for hydrogen.40

The air-fuel mixing system of an SI IC engine is shown in Figure 3. Atmospheric air is filtered first and then passes through a throttle actuator. To change AFR more accurately by the AFR controller, the fuel actuator has been designed to adjust the fuel supply. The fuel is then first purified and transferred to the fuel actuator for flow control via the fuel pump. Air and fuel mixture is then made and provided for combustion to the engine cylinders.

In the AFR control system of the IC engine, four sensors play an important role.

Throttle sensor: Often known as an air sensor. It provides the air throttle position signal to the engine control unit (ECU).

Manifold absolute pressure (MAP) sensor: It is also called a pressure sensor. It provides the suction manifold air pressure value to the ECU.

Speed sensor: It measures the speed of the engine crankshaft and provides to the ECU for controllercalculations.

Exhaust gas oxygen (EGO) sensor: It's often referred to as a gas sensor. The concentration of oxygen in the exhaust of the IC engine is measured by an EGO sensor and provided to the ECU.

In the paper, our contribution is to implement the novel HFTCS for the reliable operation of the IC engine to maintain the AFR in faulty conditions and prevent engine shutdown. In the proposed system, SMC will form the passive part to react instantly to faults while ANN will optimize post-fault performance with active compensation. Lyapunov stability analysis was performed to make sure that the system remains stable in both normal and faulty conditions. The fault tolerance is checked with noisy measurements of sen- sors to examine the robustness of the proposed control- ler. The simulation results in the Matlab/Simulink environment show that the designed controller is robust to faults in normal and noisy measurements of the sen- sors and reliable. Furthermore, the comparison with the existing works is carried out to demonstrate super- ior performance.

The structure of paper is organized as. Section ''Research methodology'' discusses the research metho- dology. Section ''Results and discussions'' presents the results and discussions. Section ''Comparison with the existing works'' elaborates on the comparison. Finally, the last section provides the conclusion of the paper.

Table 3. Model parameters.[41,42]

Parameters	Values
Engine speed	0–1000 rpm (300 rpm used in this study)
Throttle sensor range	0°–90°
MAP sensor range	0–1 bar
EGO sensor range	0–1 V
Specific heat ratio, γ	1.414

Research methodology

The proposed HFTCS is implemented on the availableIC engine model in Simulink. Mathworks explains preliminaryknowledge and model working.41,42 In thismodel, the AFR system of the gasoline engine is builtbased on the findings of Crossley and Cook43 and wasfully validated against dynamometer test data.42 Themathematical equations used for the model constructionare in accordance with the mean value enginemodel (MVEM).44 Moreover, it gives accurate AFR asfound in practical gasoline engines.40 HFTCS is a combinationof AFTCS as well as PFTCS, as previouslymentioned. AFTCS is designed using an ANN-basedobserver to build the FDI unit. In PFTCS, the AFRcontroller is designed using a robust SMC that allowssystems to manage faults without many computations.The engine speed for this study is set at 300 r/min dueto the design speed of the available MATLAB enginemodel. Therefore, a value of 300 is transmitted to thecontroller by the FDI unit in the case of a fault in thespeed sensor. We utilized constant speed in this studysince the engines in the process plant run at a constantspeed most of the time, and the designed FDI providesthe controller with 300 r/min of speed if the speed sensorfails. Because the paper is focused on designing anANN-based AFTCS system, load changes and theirimpact

on speed are not examined. The data for theMAP sensor and the throttle sensor at 300 r/min isderived using the available Matlab model lookup tables(LTs). To generate nonlinear interactions between theMAP sensor and the throttle sensor, the ANNapproach is applied. For the generation of the estimatedvalue of malfunctioning sensors, the FDI unituses these nonlinear relationships. If the throttle andMAP sensors are faulty, the FDI unit generates an estimatedvalue based on ANN observations and suppliesto the ECU. The important parameters used in themodel are mentioned in Table 3:First of all, the engine can work in its normal conditionsif there is no fault. On the other hand, if a singlesensor fault will happen, SMC will form the passivepart to react instantly to faults while ANN will optimizepost-fault performance with active compensation.Noise is introduced into the sensors, and their effect onthe output is seen in normal as well as in faultyconditions to check the robustness of the proposedHFTCS. Zero seconds have been assumed when thesensors are switched. However, a delay possibly occurs
in the switching actions. The limitations of the workare that only the full fault for sensors is carried outwithout taking partial faults which will be covered infuture works.Engine AFR system modelingThe modeling mentioned in this section is generic forcomplete theoretical analysis and adopted from wellknownliterature.40,45 The control of the air-fuel ratio isdivided into different dynamics: air dynamics, sensormodel, and fuel dynamics.Air dynamics. The dynamic manifold intake is defined bythe mass conservation theory and ideal air gas hypothesisin the following terms:

$$\dot{P}_{in} = \frac{RT_{in}}{v_{in}}\left(\dot{m}_{th} - \dot{m}_{Cyt}\right) + P_{in}\frac{\dot{T}_{in}}{T_{in}} \qquad (4)$$

$$\dot{P}_{in} = \Psi(\phi_{th}, P_{in}, T_{in}, N_e) \qquad (5)$$

Where, Pin shows manifold pressure, vin demonstrates the input volume, and Tin represents the input tempera- ture; the gas constant is R; fth illustrates the throttle opening position. The mass flow into cylinders is repre-
sented as m_ Cyt; the mass flow through the valve is demonstrated as m_ th; and engine speed is Ne. The tem- perature is assumed to be constant. Thus, equation (4) becomes:

$$\dot{P}_{in} = \dot{k}_{in}\left(\dot{m}_{th} - \dot{m}_{Cyt}\right) \qquad (6)$$

$$with \quad \dot{k}_{in} = \frac{RT_{in}}{v_{in}} \qquad (7)$$

The mass flow through the valve is:

$$\dot{m}_{th} = C_d \frac{P_{id}}{\sqrt{RT_{id}}} S_{es}(\phi_{th})\ g\ (P_r) \qquad (8)$$

Cd the coefficient of discharge. The variable Pid illustrates the pressure due to overhead loading and theload ratio Pr is the overload pressure $P_r = \frac{P_{in}}{P_{id}}$.

Thefeature Ses fð thÞ is the area of throttle opening. In animplementation, the product Cd Ses fð thÞ is consideredand also known as a single feature of throttle valveopening. It is demonstrated in several different models.The one chosen in this work is:

$$S_{e\sharp}(\phi_{th}) = C_d \quad S_{es}(\phi_{th}) = \sigma_1\{1 - \cos(\sigma_2\phi_{th} + \sigma_3)\} + \sigma_4 \qquad (9)$$

where s1=0:00051, s2=2:4357, s3=0:052, ands4=0:0011 are constants. The g(Pr) shows the nonlinearrelationship as:

$$g\ (P_r) = \begin{cases} \sqrt{\frac{2\gamma}{\gamma-1}}(P_r)^{\frac{1}{\gamma}}\sqrt{\left(1 - P_r^{\frac{\gamma-1}{\gamma}}\right)} & if \quad P_r > \left(\frac{2}{\gamma+1}\right)^{\frac{\gamma}{\gamma-1}} \\ \sqrt{\gamma}\left(\frac{2}{\gamma+1}\right)^{\frac{\gamma+1}{2(\gamma-1)}} & if \quad P_r \leqslant \left(\frac{2}{\gamma+1}\right)^{\frac{\gamma}{\gamma-1}} \end{cases} \qquad (10)$$

Fuel dynamics. It is represented as:

$$\begin{cases} \ddot{m}_{ff}(t) = \frac{1}{\tau_f}\left(-\dot{m}_{ff}(t) + x\dot{m}_{fi}(t)\right) \\ \dot{m}_{fv} = (1-x)\dot{m}_{fi}(t) \\ \dot{m}_f(t) = \dot{m}_{fv}(t) + \dot{m}_{ff}(t) \end{cases} \qquad (11)$$

Where m_ fiðtÞ represents the fuel flow injection ½kg=s————————————————, tfis the fuel vapor process, m_ fv is vapor fuel flow ½kg=s——,m€ff ðtÞ shows liquid mass fuel flow ½kg=s————, and m_ f ðtÞshows fuel flow in the cylinders ½kg=s–, , is a statevector.44 The second solution has been selected in ourcase:

$$\tau_f(N_e) = \sigma_5 N_e^{-\sigma_6} \qquad (12)$$

$$\varkappa(N_e) = \sigma_7 + \sigma_8 N_e \qquad (13)$$

Where s5, s6, s7, s8 are constant parameters. Theinjector model is given by a linear relationship betweenthe mass fuel flows from the injectors.The air-fuel ratio is then obtained:

$$\lambda_{cyl} = \frac{\dot{m}_{cyl}(t)}{\lambda_s \dot{m}_f(t)} \qquad (14)$$

00m_ cyl (t)00 is mass of cylinder, m_ f (t) is mass fuel flow intothe cylinder, ‘‘lcyl’’ is AFR in the cylinder.
Sensor model. The lambda sensor model is representedas:

$$\dot{\lambda}(t) = -\frac{1}{\tau_\lambda}\lambda(t) + \frac{1}{\tau_\lambda}\lambda_{cyl}(t - \tau(N_e(t))) \qquad (15)$$

where tl represents the time delay.The time delay t in terms of engine speed NeðtÞ isrepresented as:

$$\tau(N_e(t)) = \frac{60}{N_e(t)}\left(1 + \frac{1}{n_{cyl}}\right) \qquad (16)$$

State-space representation. It is represented as:

$$\begin{cases} \dot{x}_1 = f_1(.)x_1(t) - f_2(.)u(t) \\ \dot{x}_2 = -\frac{1}{\tau_\lambda}\lambda(t) + \frac{1}{\tau_\lambda}\lambda_{cyl}(t - \tau(N_e(t))) \end{cases} \qquad (17)$$

With $x_1(t) = \lambda_{cyl}$, $x_2(t) = \lambda(t)$, and $u(t) = \dot{m}_{fi}(t)$:

$$f_1(.) = -\frac{1}{\tau_\lambda(N_e)} - \frac{\ddot{m}_{cyl}}{m_{cyl}(N_e, P_{in})} \quad (18)$$

$$f_2(.) = \lambda_s \frac{\chi(N_e)}{\tau_f(N_e)} m_{cyl}(N_e, P_{in}) \quad (19)$$

Here "$f_1(.)$" and "$f_2(.)$" are nonlinear functions that are bounded as follows: $f_{-i} \leq f_i(.) \leq \bar{f}_i$ *for* $i \in \{1, 2\}$.

Controller design

The controller design is adopted from Sui and Hall46and given below:

$$y = u + \alpha x_1 + \beta x_2 \quad (20)$$

$$u = y_d + \alpha x_1 + \beta x_2 \quad (21)$$

Where the input is u, the output is y, and the esiredoutput is yd, the state variables are x1 and x2, engineparameters are a and b, and finally Ne is engine speed.However, in this situation, we used predicted stateobservers,

$$u = y_d + \alpha \bar{x}_1 + \beta \bar{x}_2 \quad (22)$$

where x1 and x2 are the predicted values.

$$E = \frac{1}{2}(y - \bar{y})^2 \quad (23)$$

Where the predicted output is y, the mean square erroris E. The estimated output is represented as,

$$\bar{y} = u + \alpha \bar{x}_1 + \beta \bar{x}_2 \quad (24)$$

$$E = \frac{1}{2}(y - y_d)^2 \quad (25)$$

Equation (25) shows the mean square error function,so if we take the partial derivative of the previousequation,

$$\frac{\partial E}{\partial x_1} = -\alpha(y - y_d) \quad (26)$$

$$\frac{\partial E}{\partial x_2} = -\beta(y - y_d) \quad (27)$$

The gradient descent algorithm can change the statevariables,

$$\bar{x}_1(k+1) = \bar{x}_1(k) - \eta \frac{\partial E}{\partial x_1} \quad (28)$$

$$\bar{x}_2(k+1) = \bar{x}_2(k) - \eta \frac{\partial E}{\partial x_2} \quad (29)$$

Where the estimated inputs are x1 and x2 are the predictedvalues. Adding equations (26) and (27) into the(28) and (29) we get,

$$\bar{x}_1(k+1) = \bar{x}_1(k) + \eta\alpha(y - y_d) \quad (30)$$

$$\bar{x}_2(k+1) = \bar{x}_2(k) + \eta\beta(y - y_d) \quad (31)$$

$$\therefore \eta = \frac{1}{\alpha^2 + \beta^2} \quad (32)$$

Add the value of h in the (30) and (31) equations,

$$\bar{x}_1(k+1) = \bar{x}_1(k) + \eta \frac{\alpha}{\alpha^2 + \beta^2}(y - y_d) \quad (32)$$

$$\bar{x}_2(k+1) = \bar{x}_2(k) + \eta \frac{\beta}{\alpha^2 + \beta^2}(y - y_d) \quad (33)$$

Lyapunov stability analysis is performed to check the system'sstability. Let's assume the Lyapunov function is,

$$V(x(k)) = (y_d - y)^2 \quad (34)$$

Put the values of actual and desired outputs in equation(34),

$$V(x(k)) = [\alpha(x_1(k) - \bar{x}_1(k)) + \beta(x_2(k) - \bar{x}_2(k))] \quad (35)$$

The error estimation is,

$$\tilde{x}_1(k) = (x_1(k) - \bar{x}_1(k)) \quad (36)$$

$$\tilde{x}_2(k) = (x_2(k) - \bar{x}_2(k)) \quad (37)$$

So the Lyapunov function is,

$$V(x(k)) = [\alpha\tilde{x}_1(k) + \beta\tilde{x}_2(k)] \quad (38)$$

If we change ðkÞ cycle into ðk+1Þ the cycle then theequation is,

$$V(x(k+1)) = [\alpha\tilde{x}_1(k+1) + \beta\tilde{x}_2(k+1)] \quad (39)$$

Where,

$$\tilde{x}_1(k+1) = (x_1(k+1) - \bar{x}_1(k+1)) \quad (40)$$

$$\tilde{x}_2(k+1) = (x_2(k+1) - \bar{x}_2(k+1)) \quad (41)$$

Adding equations (32) and (33) into the (40) and (41) asfollows,

$$\tilde{x}_1(k+1) = x_1(k+1) - \bar{x}_1(k) - \eta \frac{\alpha}{\alpha^2 + \beta^2}(y - y_d) \quad (42)$$

$$\tilde{x}_1(k+1) = x_2(k+1) - \bar{x}_2(k) - \eta \frac{\beta}{\alpha^2 + \beta^2}(y - y_d) \quad (43)$$

Taking the difference between actual and predicted outputis,

$$y - y_d = \alpha(x_1(k) - \bar{x}_1(k)) + \beta(x_2(k) - \bar{x}_2(k)) \quad (44)$$

$$y - y_d = \alpha\tilde{x}_1(k) + \beta\tilde{x}_2(k) \quad (45)$$

$$\bar{x}_1(k+1) = x_1(k+1) - \bar{x}_1(k) - \frac{\alpha}{\alpha^2+\beta^2}[\alpha\tilde{x}_1(k) + \beta\tilde{x}_2(k)] \quad (46)$$

$$\bar{x}_2(k+1) = x_2(k+1) - \bar{x}_2(k) - \frac{\beta}{\alpha^2+\beta^2}[\alpha\tilde{x}_1(k) + \beta\tilde{x}_2(k)] \quad (47)$$

$$x_1(k+1) = x_1(k) \quad (48)$$

$$x_2(k+1) = x_2(k) \quad (49)$$

$$\bar{x}_1(k+1) = x_1(k) - \bar{x}_1(k) - \frac{\alpha}{\alpha^2+\beta^2}[\alpha\tilde{x}_1(k) + \beta\tilde{x}_2(k)] \quad (50)$$

$$\bar{x}_2(k+1) = x_2(k) - \bar{x}_2(k) - \frac{\beta}{\alpha^2+\beta^2}[\alpha\tilde{x}_1(k) + \beta\tilde{x}_2(k)] \quad (51)$$

$$\tilde{x}_1(k+1) = \tilde{x}_1(k) - \frac{\alpha}{\alpha^2+\beta^2}[\alpha\tilde{x}_1(k) + \beta\tilde{x}_2(k)] \quad (52)$$

$$\tilde{x}_2(k+1) = \tilde{x}_2(k) - \frac{\beta}{\alpha^2+\beta^2}[\alpha\tilde{x}_1(k) + \beta\tilde{x}_2(k)] \quad (53)$$

The Lyapunov function can be written as,

$$V(x(k+1)) = \begin{bmatrix} \alpha\left[\tilde{x}_1(k) - \frac{\alpha}{\alpha^2+\beta^2}[\alpha\tilde{x}_1(k) + \beta\tilde{x}_2(k)]\right] + \\ \beta\left[\tilde{x}_2(k) - \frac{\beta}{\alpha^2+\beta^2}[\alpha\tilde{x}_1(k) + \beta\tilde{x}_2(k)]\right] \end{bmatrix} \quad (54)$$

$$V(x(k+1)) = 0 \quad (55)$$

So, the difference between both of them is,

$$V(x(k+1)) - V(x(k)) = -(y_d - y)^2 \quad (56)$$

$$V(x(k+1)) - V(x(k)) = -V(x(k)) \quad (57)$$

$$\therefore V(x(k)) = \dot{V}(x(k))$$

$$V(x(k+1)) - V(x(k)) = \dot{V}(x(k)) \quad (58)$$

The last equation shows that the difference betweenboth cycles is negative definite and hence the Lyapunovstability proof is successfully achieved. The observerdesign with ANN was already discussed in Shahbazand Amin4 for the AFTCS part.SMC mostly incorporates various control structurefeatures and facilitates non-linear processes that aresubject to large model uncertainties. SMC will form thepassive part to react instantly to faults. Consider theMIMO system,

$$\dot{x}(t) = f(x) + \sum_{i=1}^{m} g_i(x)(u_i + F_i(x,t)) \quad (59)$$

$$y_i = h_i(x) \quad (60)$$

Where u represents the input, x shows the state vector,and y is the output of the system. f ðxÞ and giðxÞ arevector fields, and hiðxÞ is a smooth function. Fiðx, TÞdemonstrates the uncertainty and it is further classifiedinto structured and unstructured parts:

$$F_i(x,t) = \vartheta_{si} + \vartheta_{ui}(x,t) \quad (61)$$

Where qsi is partial uncertainty and it is written as,

$$\vartheta_{si}(x) = \Delta_i \Xi_i(x) \quad (62)$$

Consider sliding surface:

$$S_i = S_{oi}(x) + z_i \quad (63)$$

Where S_i, $S_{oi}(x)$, and $z_i \in \mathbb{R}^m$. S_i is a sliding variable, and S_{oi} is a conventional sliding mode design. The structure of sliding surfaces is controlled by:

$$\dot{S}_i = \frac{\partial S_{oi}}{\partial x_i}\left[f_i(x) + \sum_{k=1}^{m} g_k(x)\{u_k + F_k(x,t)\}\right] + \dot{z}_i \quad (64)$$

$$\dot{S}_i = \frac{\partial S_{oi}}{\partial x_i} f_i(x) + \frac{\partial S_{oi}}{\partial x_i}\sum_{k=1}^{m} g_k(x)\{u_k + F_k(x,t)\} + \dot{z}_i \quad (65)$$

We can write as:

$$\dot{S} = N(x) + G(x)(U + F) + \dot{Z} \quad (66)$$

Where $N(x) = \left[\frac{\partial S_{o1}}{\partial x_1} f_1(x), \ldots, \frac{\partial S_{om}}{\partial x_m} f_m(x)\right]^T$, $\dot{Z} = [\dot{z}_1, \ldots, \dot{z}_m]^T$, $G(x) = [G_1(x), \ldots, G_m(x)]^T$, and $G_i(x)(U+F) = \frac{\partial S_{oi}}{\partial x_i}\sum_{k=1}^{m} g_k(x)\{u_k + F_k(x,t)\}$. Taking:

$$U = U_o + \bar{U} \quad (67)$$

Where Uo maintain the known terms, and Uo managethe uncertain terms and actuators' faults. Assume thatG1ðxÞ exists and taking Uo as:

$$U_o = G^{-1}(x)\{-N(x)\} \quad (68)$$

Where Uo provides the desired output and eliminates alluncertainties and faults as well. Taking _Z as:

$$\dot{Z} = -N(x) - G(x)U_o \quad (69)$$

The remaining system can be handled over:

$$\dot{S}_i = F_i + \bar{u}_i \quad (70)$$

$$\dot{S}_i = \Delta_i \Xi_i(x) + \vartheta_{ui}(x,t) + \bar{u}_i \quad (71)$$

Unstructured uncertainties are assumed to be handledas:

$$|\vartheta_{ui}(x,t)| \leq \Omega |S_i(x)|^{\frac{1}{2}} \quad (72)$$

The controller structure ui is taken as:

$$\bar{u}_i = -M_i|S_i|^{\frac{1}{2}}\,sign(S_i) - \hat{\Delta}_i\Xi_i(x) \quad (73)$$

The Lyapunov function is used to get adaptation laws of unknown parameters (Δ_i):

$$V = \sum_{i=1}^{m}\left[|S_i| + \frac{1}{2\gamma_i}\hat{\Delta}_i^{\,2}\right] \quad (74)$$

Where $\gamma_i>0$. Consider now the time derivative of the Lyapunov function (74).

$$\dot{V} = \sum_{i=1}^{m}\left[sign(S_i)\dot{S}_i + \frac{1}{\gamma_i}\widetilde{\Delta}_i\dot{\hat{\Delta}}_i\right]\sum \quad (75)$$

Using equations (71) to (73) in (75).

$$\dot{V} = \sum_{i=1}^{m}\left[sign(S_i)\left\{\vartheta_{ui}(x,t) - M_i|S_i|^{\frac{1}{2}}sign(S_i) - \left(\hat{\Delta}_i - \Delta_i\right)\Xi_i(x)\right\} + \frac{1}{\gamma_i}\tilde{\Delta}_i\dot{\hat{\Delta}}_i\right] \quad (76)$$

$$\therefore \dot{V} = \sum_{i=1}^{m}\left[sign(S_i)\left\{\Omega_i|S_i|^{\frac{1}{2}} - M_i\,|S_i|^{\frac{1}{2}}\right\} + \tilde{\Delta}_i\left\{-sign(S_i)\Xi_i(x) + \frac{1}{\gamma_i}\dot{\hat{\Delta}}_i\right\}\right] \quad (77)$$

If $\hat{\Delta}_i s$ are exactly known, then $\tilde{\Delta}_i = 0$ and $\dot{V}$ becomes:

$$\dot{V} \leqslant \sum_{i=1}^{m}\left[|S_i|^{\frac{1}{2}}\,sign(S_i)\{\Omega_i - M_i sign(S_i)\}\right] \quad (78)$$

Selecting $M_i>\Omega_i$, $\dot{V}$ becomes negative. But $\hat{\Delta}_i s$ are not known perfectly, hence choosing the adaptation laws as:

$$\dot{\hat{\Delta}}_i = \gamma_i sign(S_i)\Xi_i(x) \quad (79)$$

We have:

$$\therefore \dot{V} \leqslant \sum_{i=1}^{m}\left[|S_i|^{\frac{1}{2}}\,sign(S_i)\{\Omega_i - M_i sign(S_i)\}\right] \quad (80)$$

Lyapunov stability analysis in equation (80) provides the best-estimated values of faults and does not require any constraints on structured disturbances.

The non-linear model of the IC engine described earlier provides the most important properties of the proposed controller. From the previous equation (4) of air dynamics, we can write as:

$$\dot{P}_{in} = \frac{RT_{in}}{v_{in}}\left(\dot{m}_{th} - \dot{m}_{Cyt}\right) + P_{in}\frac{\dot{T}_{in}}{T_{in}}$$

Where $k_{in} = \frac{RT_{in}}{v_{in}}$

$$\dot{P}_{in} = k_1\left(\dot{m}_{Cyt} - u_1 - P_{id}\right) \quad (81)$$

$$P_{id} = k_2\left(\dot{m}_{Cyt} - u_2 - u_1\right) \quad (82)$$

Where u1 and u2 is control inputs and k1 and k2 is massflows. The output as set point regulation errors areselected as:

$$y_1 = \dot{m}_{Cyt} - \dot{m}^d{}_{Cyt} \quad (83)$$

Where $\dot{m}^d{}_{Cyt}$ is the desired mass flow into the cylinder.

$$y_2 = \dot{P}_{id} - \dot{P}^d{}_{id} \quad (84)$$

Where $\dot{P}^d{}_{id}$ is desired overloading manifold pressure. Input-output linearization of output equations (83) and (84), put in equations (81) and (82) gives:

$$\dot{y}_1 = -\left(\frac{\dot{m}_{Cyt}}{\tau}\right) - a\left(\dot{m}_{Cyt} - k_{in}\dot{P}_{in}\right) + bu_2 - au_1 \quad (85)$$

$$\dot{y}_2 = k_2\left(k_{in}\dot{P}_{in} + \dot{m}^d{}_{Cyt}\right) - k_2u_1 - k_2u_2 \quad (86)$$

Control law:

The derivatives of the sliding variables after takinginto account structured and unstructured uncertaintiesare:

$$\dot{S}_1 = -\left(\frac{\dot{m}_{Cyt}}{\tau}\right) - a\left(\dot{m}_{Cyt} - k_{in}\dot{P}_{in}\right) + bu_2 - au_1 - \Theta_1 - \vartheta u_1 + \dot{z}_1 \quad (87)$$

$$\dot{S}_2 = k_2\left(k_{in}\dot{P}_{in} + \dot{m}^d{}_{Cyt}\right) + k_2u_2 - k_2u_1 - \Theta_2 - \vartheta u_2 + \dot{z}_2 \quad (88)$$

Here, Yi represents the structured faults. These structuredfaults can be represented in terms of flow rates:

$$\Theta_1 = \Delta_1\Xi_1(x) = \Delta_1\dot{m}_{Cyt} \quad (89)$$

$$\Theta_2 = \Delta_2\Xi_2(x) = \Delta_2\dot{m}_{th} \quad (90)$$

Where Y1 and Y2 represents the over and under-flowthrough exhaust gas recirculation and variable geometryturbo actuators respectively. It is assumed thatunstructured uncertainties are bounded:

$$|\vartheta_{u1}(x,t)| \leqslant \Omega_1|S_1(x)|^{\frac{1}{2}}, \quad \Omega_1>0 \quad (91)$$

$$|\vartheta_{u2}(x,t)| \leqslant \Omega_2|S_2(x)|^{\frac{1}{2}}, \quad \Omega_2>0 \quad (92)$$

The control action is proposed in equation (67). Towork out uoi (control that can stabilize unaffectedplant), ignoring structured faults, and unstructuredfaults in equations (85) and (86):

$$\dot{S}_{o1} = -\left(\frac{\dot{m}_{Cyt}}{\tau}\right) - a\left(\dot{m}_{Cyt} - k_{in}\dot{P}_{in}\right) + bu_2 - au_1 - \Theta_1 - \vartheta u_1 + \dot{z}_1 \quad (93)$$

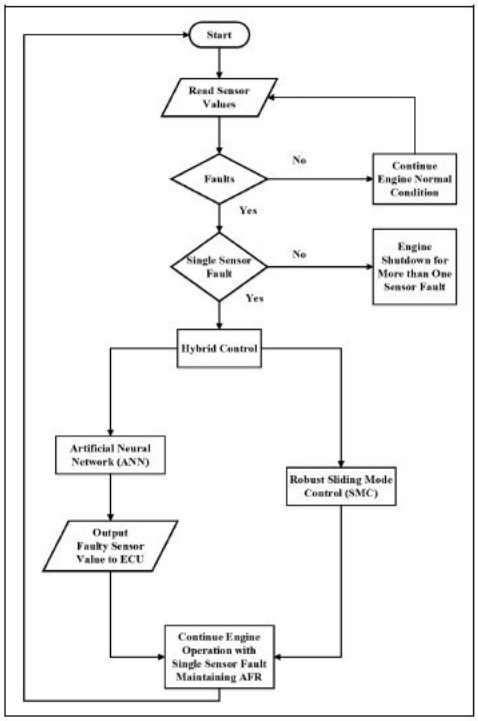

Figure 4. Proposed model of HFTCS.

$$\dot{S}_{o2} = k_2\left(k_{in}\dot{P}_{in} + \dot{m}^d{}_{Cyt}\right) + k_2u_2 - k_2u_1 - \Theta_2 - \vartheta u_2 + \dot{z}_2 \tag{94}$$

For ideal plant:

$$u_{o1} = \frac{1}{a+b}\left[-\dot{m}_{Cyt}\left(a + \frac{1}{\tau}\right) + (a+b)k_{in}\dot{P}_{in} + b\dot{m}^d{}_{Cyt}\right] \tag{95}$$

$$u_{o2} = \frac{1}{a+b}\left[-\dot{m}_{Cyt}\left(a + \frac{1}{\tau}\right) + b\dot{m}^d{}_{Cyt}\right] \tag{96}$$

Results and Discussions

For fault detection, isolation, and reconfiguration ofcontrollers, FDI is implemented in the model withANN. The FDI unit continuously tracks the sensorvalues for any fault. If the sensor value exceeds thespecified limit, a fault is detected by threshold

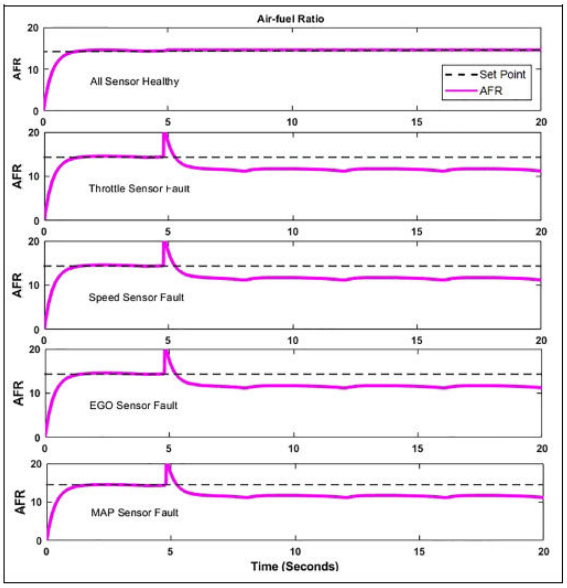

Figure 5. Performance of AFTCS.

comparison. Once the fault has been observed, an estimatedvalue of the observer model based on ANN issubstituted for the fault value and is supplied to theECU. The active part performs post-fault optimal performancefor the active compensation by providing theestimated value of the faulty sensor by ANN observerusing the other healthy sensors. Two ANNs have beenintroduced for throttle and MAP sensors. Since theengine is running at 300 r/min, this value has been suppliedto the controller if a fault occurs in the speed sensor.The AFTCS portion is simulated with sensor faultsone at a time and the effects on the AFR are observedat t=5 s due to the internal warm-up delay of theengine, as shown in Figure 5. Results from Figure 5show that the AFR is constantly degraded to 11.7 with
every single sensor fault on the AFTCS portion alone.The passive part of the system consists of robustSMC. It provides a very quick response against fault,and after a very minor glitch in the output, the systemmaintains its steady state. Since the AFR decreases to11.7 in the AFTCS part, the SMC controller with a fuelactuator is designed to keep it to 14.6 in faultyconditions.

In each of the four sensors, the faults are inserted att=0 s, and the results on the AFR are detected att=5 s due to internal warm-up times of 5 s in the originalmodel. Figure 6 shows the results achieved for eachsensor without noise in the sensors. The outputresponse of the proposed PFTCS for faults in each sensoris demonstrated in Figure 6. In the existing model,AFR is affected by faults in each sensor and decreases
to 11.7, that is, degradation in the performance infaulty conditions. However, the proposed PFTCSmaintains AFR to 14.6 in normal as well as faultyconditions.These results show that the proposed PFTCS isrobust to single-sensor faults.The performance of the overall HFTCS for the foursensors is shown in Figure 7 in normal and faulty conditions.The system maintains an AFR of 14.6 in faultysituations, according to the results. The proposedHFTCS is resistant to sensor faults, preserving its performanceand thereby avoiding AFR degradation. Theresults represent that after a very minor glitch, the systemmaintains its steady state with the help of a robustSMC controller. Table 4 illustrates the robustness of

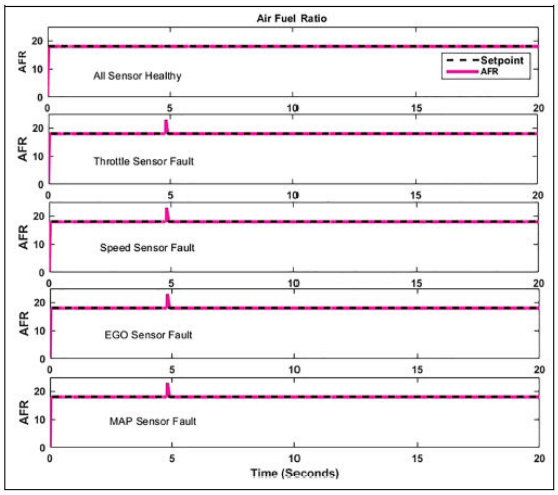

Figure 6. Performance of PFTCS.

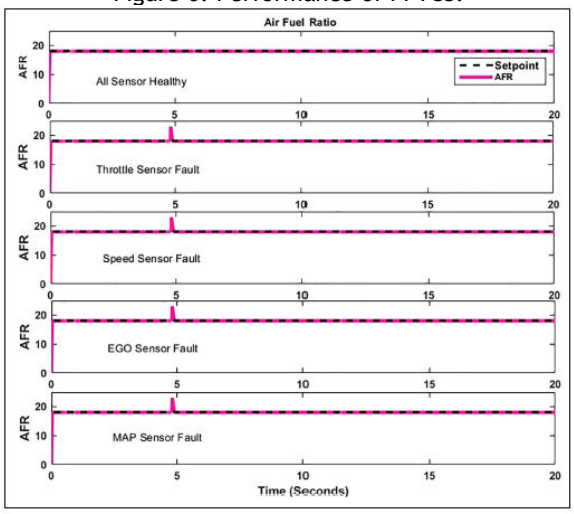

Figure 7. Performance of HFTCS without noise.

Table 4. Performance of Proposed HFTCS without noise introduced.

Faulty sensor	AFR	Stability issue
Throttle sensor	No effect on AFR	AFR is stable
Speed sensor	No effect on AFR	AFR is stable
MAP sensor	No effect on AFR	AFR is stable
EGO sensor	No effect on AFR	AFR is stable

Table 5. Parameters of noise for sensors.

Parameters of noise	MAP and EGO	Speed and throttle
Seed	[23341]	[23341]
Sampling time	0.1	0.1
Noise power	0.0001	0.01

Table 5. Parameters of noise for sensors.

Parameters of noise	MAP and EGO	Speed and throttle
Seed	[23341]	[23341]
Sampling time	0.1	0.1
Noise power	0.0001	0.01

the proposed HFTCS with ANN and SMC withoutnoisy conditions of sensors.After confirming adequate efficiency in noise-freeoperation, the system response is tested by integratingnoise into sensor measurements. Table 5 shows thenoise parameters introduced in the sensors. Greaternoise is incorporated for throttle and speed sensor measurementsdue to high sensor values. Due to the verylimited range, smaller noise is added in sensors EGOand MAP. In Figure 8, the effects of AFR are illustratedin normal and faulty conditions. The resultsdemonstrated that after very minor sparks in the output,the system achieves the set point even under faultyconditions. The AFR remains stable with small misfiresand the system continues to operate successfully in thenoisy conditions of sensors. The performance of theproposed HFTCS with noise introduced is shown inTable 6.The output response in Figure 8 is dominated by thePFTCS that is running in parallel with AFTCS. Theactive part performs post-fault optimal performancefor the active compensation by providing the estimatedvalue of the faulty sensor by ANN observer using the other healthy sensors. Since both controllers work inparallel, the active compensation effect does notbecome much evident due to the dominance of the passivecontroller. However, it becomes very much evidentin only active FTCS as shown in Figure 5.

Comparison with the existing works

In this section, a comparison of the proposed HFTCSwith the existing models is discussed. We have designedan HFTCS with dedicated non-linear controllers

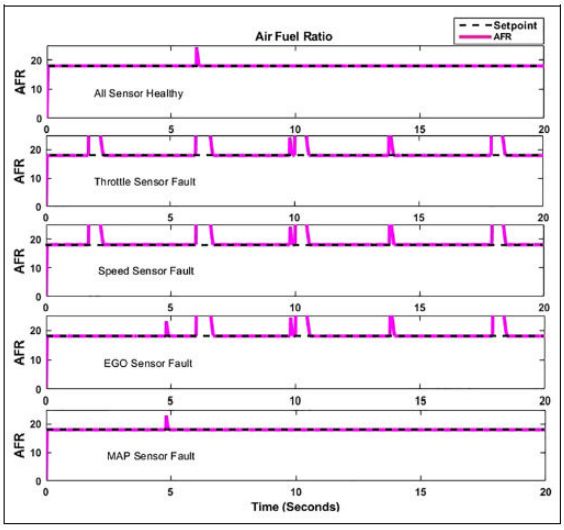

Figure 8. Performance of HFTCS in noisy conditions.

Table 6. Performance of Proposed HFTCS with noise introduced.

Faulty sensor	AFR	Stability issue
Throttle sensor	No effect on AFR	AFR is stable
Speed sensor	No effect on AFR	AFR is stable
MAP sensor	No effect on AFR	AFR is stable
EGO sensor	No effect on AFR	AFR is stable

known as ANN and SMC. The previous work has notused the ANN and SMC together for HFTCS designfor the AFR system of the IC Engine. In the proposedsystem, SMC will form the passive part to reactinstantly to faults while ANN will optimize post-faultperformance with active compensation. Moreover,Lyapunov stability analysis was performed to makesure that the system remains stable in both normal andfaulty conditions. The estimated values of the throttleand MAP sensors, as well as the accompanying meansquare errors (MSE), are shown in Shahbaz andAmin.4 ANN approach can cover the complete nonlinearrange of the MAP sensor, which is also less computationally expensive than lookup tables and hencepreferred. Due to its valuable functionalities of learning,self-organization, and non-linear modeling capabilities,the ANN technique is currently becoming apreferred strategy in fault diagnostics.In Amin and Mahmood-ul-Hasan,14 the HFTCSwas proposed with Kalman Filters in the active partand a high-gain PI controller in the passive part. Thisalgorithm was limited to the linear range of the highlynonlinear sensors of the AFR control system. In Suet al.,15 the HFTCS was proposed for the sensors ofthe distillation column without using any intelligent control or data-driven technique. In Wang et al.,16 theHFTCS was proposed for the uncertain networkedcontrol systems under a discrete event-triggered communicationscheme that was not applied to the processplant. In Yang et al.,48 the authors focused on faulttolerantcontrol of Markov

jump systems (MJS) withIto^ stochastic process and output disturbances. Aproportional-derivative sliding mode observer (SMO)and an observer-based controller are first devised andfabricated. In Yang et al.,49 the authors provided afault-tolerant compensation control strategy forMarkov jump systems against nonlinearity, simultaneousadditive, and multiplicative actuator failures. Afuzzy logic system (FLS) was used to estimate the nonlinear functions and by using the adaptive backsteppingapproach, an FLS-based adaptive fault-tolerant compensationcontroller is developed. The proposed methodsworked very well for the stochastic disturbancesand simultaneous additive and multiplicative typefaults in the actuators. However, the stochastic delaysand actuator faults were not studied in this paper.The proposed HFTCS has PFTCS for AFR control,which is based on SMC, and AFTCS based on ANN.With the use of a fuel throttle actuator, the proposedHFTCS will compensate for the AFR degradation bythe AFR control. In the proposed system, SMC will form the passive part to react instantly to faults whileANN will optimize post-fault performance with activecompensation as shown in Figure 5. The previousworks mentioned in the literature have not yet utilizedany intelligent control technique like ANN for theAFTCS and regular sliding mode control for thePFTCS, as proposed in this paper. The proposed modelwas found to be robust to faults in the normal andnoisy conditions of the sensors. Therefore, the proposedHFTCS with ANN and SMC presents an optimum andreliable solution for AFR control in SI IC engines.Table 7 provides a comprehensive comparison of thesuggested strategy with previously used strategies.

Table 7. Comparison of proposed HFTCS with previous works.[4,14,50–53]

Name of controller	Major drawback	Chattering reduction	Degree of robustness	Response against noise
Proposed HFTCS	Misfires	Can be further improved with advanced SMC	High	Relatively low misfiring observed
HFTCS based on Kalman filter	Linear range of sensors	Does not eliminate chattering	Moderate	High misfiring observed
HFTCS based on GA and HOSMC	Oscillations in AFR transient response	Better	High	High misfiring observed
HFTCS based on FLC and HOSMC	Oscillations in AFR transient response	Better	High	High misfiring observed
AFTCS based on ANN and FLC	Performance degradation	Does not eliminate chattering	Unknown duration for handling faults	High misfiring observed
AFTCS based on non-linear regression	Performance degradation	Does not eliminate chattering	Not a robust technique	High misfiring observed

Conclusions

In conclusion, this study successfully demonstrates the effectiveness of integrating artificial neural networks (ANNs) with sliding mode control (SMC) for managing the air-fuel ratio in internal combustion engines (ICEs) while ensuring robustness against sensor failures. The proposed hybrid control strategy not only enhances the precision of air-fuel ratio predictions but also maintains system stability and performance in the presence of potential sensor malfunctions. The ANN's ability to learn from varying engine operating conditions allows for adaptive and responsive control, significantly improving combustion efficiency and reducing harmful emissions. Meanwhile, the SMC framework effectively mitigates the adverse effects of sensor inaccuracies, ensuring consistent engine operation. Simulation results confirm that this innovative approach outperforms traditional control methods, offering a reliable solution to the challenges posed by sensor uncertainties. This research contributes valuable insights into advanced control strategies for ICEs, paving the way for the development of smarter, more efficient automotive technologies that align with the industry's goals for sustainability and reduced environmental impact. Future work should focus on real-world implementation and further refinement of the proposed system to address additional complexities in engine dynamics and operational conditions.

Funding

The author(s) received no financial support for the research,authorship, and/or publication of this article.

References

1. Jiang J. Fault-tolerant control Systems: an introductory overview1. Zidonghua Xuebao 2005; 31: 14.
2. Frank PM. Trends in fault-tolerant control of engineer- ing systems. IFAC Proc Volumes 2004; 37: 377–384.
3. Amin AA and Hasan KM. A review of fault tolerant control systems: advancements and applications. Mea- surement 2019; 143: 58–68.
4. Shahbaz MH and Amin AA. Design of active fault toler- ant control system for air fuel ratio control of internal combustion engines using artificial neural networks. IEEE Access 2021; 9: 46022–46032.
5. Amin AA and Mahmood-ul-Hasan K. Robust active fault-tolerant control for internal combustion gas engine for air–fuel ratio control with statistical regression-based observer model. Meas Control 2019; 52: 1179–1194.
6. Jiang J and Yu X. Fault-tolerant control systems: A comparative study between active and passive approaches. Annu Rev Control 2012; 36: 60–72.
7. Mahmoud M and Xia Y. Industrial fault-tolerant archi- tectures. In: Analysis and synthesis of fault-tolerant con- trol systems. Chichester: John Wiley & Sons, Ltd, 2013, 307–319.
8. Ahmed S, Amin AA, Wajid Z, et al. Reliable speed control of a permanent magnet DC motor using fault-tolerant H-bridge. Adv Mech Eng 2020; 12: 1687814020970311.
9. Benosman M. Passive fault tolerant control. Cambridge: IntechOpen, 2011.

10. Amin AA and Mahmood-Ul-Hasan K. Advanced Fault Tolerant Air-fuel ratio control of internal combustion gas engine for sensor and actuator faults. IEEE Access 2019; 7: 17634–17643.
11. Amin AA and Mahmood-ul-Hasan K. Robust passive fault tolerant control for air fuel ratio control of internal combustion gasoline engine for sensor and actuator faults. IETE J Res 2021; 1–16.
12. Blanke M, Staroswiecki M and Wu NE. Concepts and methods in fault-tolerant control. In: Proceedings of the 2001 American Control Conference (cat. no. 01CH37148), Arlington, VA, USA, 2001, vol. 4, pp.2606–2620.
13. Yuan Y, Liu X, Ding S, et al. Fault detection and loca- tion system for diagnosis of multiple faults in aeroen- gines. IEEE Access 2017; 5: 17671–17677.
14. Amin AA and Mahmood-ul-Hasan K. Hybrid fault toler- ant control for air–fuel ratio control of internal combus- tion gasoline engine using Kalman filters with advanced redundancy. Meas Control 2019; 52: 473–492.
15. Su SW, Bao J and Lee PL. A hybrid active–passive fault- tolerant control approach. Asia Pac J Chem Eng 2006; 1: 54–62.
16. Wang J, Yao X and Li W. Hybrid active-passive robust fault-tolerant control of event-triggered nonlinear NCS. Open Electr Electron Eng J 2017; 11: 68–86.
17. Li L. Fault detection and fault-tolerant control for non- linear systems. Wiesbaden: Springer Fachmedien Wiesba- den, 2016.
18. Yang H, Jiang B and Cocquempot V. Fault tolerant con- trol design for hybrid systems, vol. 397. Berlin, Heidelberg: Springer Berlin Heidelberg, 2010..
19. Tang L, Ma D and Zhao J. Neural networks-based active fault-tolerant control for a class of switched nonlinear sys- tems with its application to RCL circuit. IEEE Trans Syst Man Cybern 2018; 50: 4270–4282. https://ieeexplore.ieee.org/document/8409459
20. Patel HR and Shah V. Fuzzy logic based passive fault tolerant control strategy for a single-tank system with system fault and process disturbances. In: 2018 5th inter- national conference on electrical and electronic engineering (ICEEE), Istanbul, Turkey, 2018, pp.257–262.